Gas-Phase Reactions Between Thiourea and Ca2+: New Evidence for the Formation of [Ca(NH3)]2+ and Other Doubly Charged Species

ARTICLE *in* CHEMPHYSCHEM · JUNE 2007

Impact Factor: 3.42 · DOI: 10.1002/cphc.200700113 · Source: PubMed

5 AUTHORS, INCLUDING:

Cristina Trujillo
Trinity College Dublin
36 PUBLICATIONS **395** CITATIONS
SEE PROFILE

Otilia Mó
Universidad Autónoma de Madrid
403 PUBLICATIONS **6,379** CITATIONS
SEE PROFILE

Manuel Yanez
Universidad Autónoma de Madrid
271 PUBLICATIONS **3,747** CITATIONS
SEE PROFILE

Jean-Yves Salpin
Université d'Évry-Val-d'Essonne
147 PUBLICATIONS **1,344** CITATIONS
SEE PROFILE

CHEMPHYSCHEM

DOI: 10.1002/cphc.200700113

Gas-Phase Reactions Between Thiourea and Ca^{2+}: New Evidence for the Formation of $[Ca(NH_3)]^{2+}$ and Other Doubly Charged Species

Cristina Trujillo,[a] Otilia Mó,[a] Manuel Yáñez,*[a] Jean-Yves Salpin,*[b] and Jeanine Tortajada[b]

The gas-phase reactions between Ca^{2+} and thiourea are investigated by means of electrospray ionization/mass spectrometry experiments. The MS/MS spectra of $[Ca(thiourea)]^{2+}$ complexes show the appearance of new doubly charged species formed by the loss of NH_3 and HNCS. Other intense peaks at m/z *43, 56, 60, 73, 76 and 98 are also observed, and assigned to monocations produced in different coulomb-explosion processes. The structures and bonding characteristics of the different stationary points of the $[Ca(thiourea)]^{2+}$ potential energy surface (PES) were theoretically studied by DFT calculations carried out at B3LYP/cc-pWCVTZ level. The analysis of the topology of this PES permits to propose different mechanisms for the loss of ammonia and HNCS, and to identify, the* m/z *43, 56, 60, 73, 76 and 98 peaks as H_2NCNH^+, $CaNH_2^+$, H_2NCS^+, $CaSH^+$, $thiourea^{+\cdot}$ and $CaNCS^+$ ions respectively. There are significant dissimilarities between the reactivity of urea and thiourea, which are related to the lower ionization energy of the latter, and to the fact that thioenols are intrinsically more stable than enols with respect to the corresponding keto forms.*

Introduction

Most of the experiments in gas-phase ion chemistry deal with singly charged species. However, in recent years, due to the development of electrospray ionization (ESI) techniques, the number of studies on the interaction of divalent cations with neutral molecules in the gas-phase has grown significantly.[1–27] Although monosolvated dications, such as $Cu(H_2O)^{2+}$, $Cu(NH_3)^{2+}$ or $Pb(H_2O)^{2+}$, have been detected in the gas phase,[6,18,25] and their lifetimes have been predicted to be extremely large when they are in the lower vibrational states,[28] most of the doubly charged species formed by association of a dication to a neutral system are stabilized through the interaction with several neutral or solvent molecules, so in some cases there is a critical minimum size of the cluster for the multiply charged species to be detected by usual mass spectrometry techniques. As a matter of fact, when dealing with transition metal dications, the simple adducts ML^{2+} in which the metal associates with a single neutral molecule are very often not seen. This is the case for instance when dealing with Cu^{2+} and different bases. The oxidative character of the metal dication leads to the formation of the corresponding ligand radical cation $L^{+\cdot}$, which exhibits a much greater acidity than the neutral system. Consistently, what it is detected in the gas phase are the $[(L–H)M]^+$ monocations produced by the deprotonation of this radical cation.

This is not the case however when dealing with alkaline-earth dications such as Ca^{2+}. The recombination energy of Ca^{2+} is much smaller than those of most of the transition metal dications (the second ionization energy being much smaller for Ca than for most of the transition metals) and therefore its oxidative character much smaller. The consequence is that CaL^{2+} dications may be detected in the gas phase. This is indeed the case when the ligand is urea[29] or the first aminoacid, glycine.[30] This finding prompted us to initiate a systematic investigation of the reactions of Ca^{2+} with different bases of biochemical relevance, since the importance of divalent alkaline-earth metal dications (Mg^{2+}, Ca^{2+}, Ba^{2+}) in many biological processes is well established.[31–35]

Previous investigations have shown[29] that in the reactions between Ca^{2+} and urea, coulomb explosions play a crucial role, although also new doubly charged species, such as H_3NCa^{2+} and $HNCOCa^{2+}$, are produced in the reactions through unimolecular fragmentations, in which HNCO and neutral ammonia, respectively are lost. Interestingly, replacing an amino group by a hydroxyl group in the base, which is the difference between urea and glycine, changes the reactivity

[a] C. Trujillo, Prof. O. Mó, Prof. M. Yáñez
Departamento de Química, C-9. Universidad Autónoma de Madrid
Cantoblanco, 28049 Madrid (Spain)
Fax: (+34) 91-497-5238
E-mail: manuel.yanez@uam.es

[b] Dr. J.-Y. Salpin, Prof. J. Tortajada
Laboratoire Analyse et Modélisation pour la Biologie et l'Environnement
Université d'Evry Val d'Essonne, CNRS
Bâtiment Maupertuis, Boulevard François Mitterrand
91025 Evry (France)
Fax: (+33) 1-69-47-76-55
E-mail: jean-yves.salpin@univ-evry.fr

Supporting information for this article is available on the WWW under http://www.chemphyschem.org or from the author.

pattern completely and only coulomb explosions are observed experimentally.[30] The aim of this paper is to investigate the reactivity pattern when the basic site of the system is a second-row atom by studying the reactions of Ca^{2+} with thiourea (**TU**). Besides, like urea, thiourea has an undoubted relevance from the biological point of view. As a matter of fact, thiourea itself influences the photosynthesis of some species,[36] protects against oxidative damage[37,38] and some of its derivatives behave as radical scavengers[39] or inhibit virus replication.[40–42] Therefore, investigating whether the intrinsic reactivity of thiourea versus Ca^{2+} exhibits some peculiarities with respect to that shown by urea, is of great interest.

To get a complete picture of these reactivity patterns it is useful to combine the experimental information on the products distribution obtained by means of mass spectrometry techniques with a theoretical survey on the bonding and on the topology of the potential energy surface (PES) that connects the reactants with the products. For this purpose, in a previous paper[43] we have carried out an assessment of theoretical procedures for the description of the interactions between neutral molecules and Ca^{2+}. In that paper we have concluded that the B3-LYP density functional method associated with a cc-pWCVTZ basis set expansion provides a good compromise between accuracy and computational cost in the calculation of structures and binding energies for Ca^{2+} complexes. Hence, this is the theoretical scheme used herein, in combination with electrospray ionization mass spectrometry experiments.

Experimental and Computational Methods

Electrospray mass spectra were recorded on a QSTAR PULSAR i (Applied Biosystems/MDS Sciex) hybrid instrument (QqTOF) fitted with a nanospray source to minimize transfer-line contamination. Several μL of aqueous mixtures of calcium chloride ($5x10^{-4}$ mol L^{-1}) and thiourea (10^{-4} mol L^{-1}) were nanosprayed (20–50 nL min^{-1}) using borosilicate emitters (Proxeon). Samples were ionized using a 900 V nanospray needle voltage and the lowest possible nebulizing gas pressure (tens of millibars). The declustering potential (DP, also referred to as "cone voltage"), defined as the difference in potentials between the orifice plate and the skimmer (grounded), ranged from 0 to 40 V. The operating pressure of curtain gas (N_2) was adjusted to 0.7 bar by means of an electronic board (pressure sensors), as a fraction of the N_2 inlet pressure. To improve ion transmission and subsequently sensitivity during the experiments, collision gas (CAD, N_2) was present at all times for collisional focusing in both the Q0 (ion guide preceding Q1 and located just after the skimmer) and Q2 (collision cell) sectors. For MS/MS spectra, ions of interest were mass selected using quadrupole Q1, and allowed to collide with nitrogen gas at various collision energies ranging from 8 eV to 14 eV in the laboratory frame (the collision energy is given by the difference between the potentials of Q0 and Q2), with the resulting fragments separated by the time-of-flight (TOF) analyzer after orthogonal injection. Low gas pressures (typically 1–2 10^{-5} mbar) were used to limit multiple ion–molecule collisions. Thiourea and calcium salt were purchased from Aldrich and were used without further purification. All the measurements presented hereafter were carried out in 100% water purified with a Milli-Q water purification system.

Computational Details: The geometries of neutral thiourea as well as those of the different stationary points of the $[Ca(\mathbf{TU})]^{2+}$ potential energy surface were optimized using the B3LYP[44,45] density functional theory (DFT) approach, combined with cc-pWCVTZ[46,47] basis sets, which includes core-correlation functions which are important for the accurate treatment of alkaline earth metal oxides and hydroxides, as well as for the accurate calculation of Ca^{2+} binding energies.[43] The same theoretical scheme has been used to obtain their harmonic vibrational frequencies, used to classify the stationary points found as local minima or transition states, and to estimate the corresponding zero-point energy (ZPE) corrections, which were scaled by the empirical factor 0.985.[48] To assess the connectivity between each transition state and the minima to which it evolves we have used the intrinsic reaction coordinate (IRC) procedure as implemented in the Gaussian 03 suite of programs.[49]

Binding energies were calculated, at the same levels of theory used for geometry optimizations, as the difference between the energy of the most stable $[Ca(\mathbf{TU})]^{2+}$ complex and the energy of urea, in its most stable conformation and the energy of Ca^{2+}, after including the ZPE corrections.

The bonding within the different local minima was analyzed by evaluating the molecular graph of the most stable $[Ca(\mathbf{TU})]^{2+}$ and by calculating the corresponding energy density contour map, within the framework of the atoms in molecules (AIM) theory.[50] The relative changes in the charge density at the different bond critical points give information on the bonding perturbation undergone by the base, upon Ca^{2+} association. On the other hand, the sign of the energy density within each bonding region clearly indicates the covalent or ionic nature of the interaction.

Results and Discussion

Mass Spectrometry

For thiourea, the experimental conditions allowing the doubly-charged complex to be observed with a significant abundance are different from those adopted for the Ca^{2+}/urea system. First, a very low cone voltage (DP = 0 V) had to be used. Regardless of the DP value, the overwhelming species is the calcium hydroxide $CaOH^+$ species (*m/z* 57). An ion at *m/z* 75, attributed to $CaOH^+$. H_2O is also observed in significant abundance. Interaction between thiourea and calcium ion gives rise to both singly- and doubly-charged complexes. Only one doubly-charged adduct, namely the $[Ca(thiourea)]^{2+}$ ion (*m/z* 58), is detected with a relative abundance of c.a. 10%. However, even with the DP parameter set to 0 V, its observation is not straightforward and preliminary optimization of the metal: thiourea ratio was necessary. This is achieved by varying the concentration of the metal while keeping that of thiourea constant (10^{-4} mol L^{-1}), the DP value being fixed at 0 volts. In these conditions, the highest intensity of the *m/z* 58 ion has been obtained with a 5:1 ratio. Singly charged complexes of general formula $[Ca(\mathbf{TU})_n{-}H]^+$ ($n = 1$–3) are detected at *m/z* 115, 191 and 267. An additional intense ion corresponds to protonated thiourea (*m/z* 77).

Increasing the DP results in significant changes in the electrospray spectrum. First, the $[Ca(thiourea)]^{2+}$ complex quickly disappears. While $CaOH^+$ remains the base peak, increasing

the cone voltage induces various in-source fragmentation processes. As a matter of fact, the $[Ca(\mathbf{TU})_2{-}H]^+$ (*m/z* 191) and $[Ca(\mathbf{TU})_3{-}H]^+$ (*m/z* 267) dissociate according to elimination of intact **TU** units, as checked by complementary MS/MS experiments. This results in the small increase of the intensity of the $[Ca(\mathbf{TU}){-}H]^+$ ion (*m/z* 115). In turn, this latter species eliminates a molecule of ammonia to give rise to a peak at *m/z* 98. A similar process occurs from protonated thiourea, resulting in an intense *m/z* 60 ion at high DP. Note that both *m/z* 60 and 98 ions could also correspond to dissociation of the doubly charged $[Ca(thiourea)]^{2+}$ ion, as detailed below.

We will now focus on the $[Ca(\mathbf{TU})]^{2+}$ MS/MS spectra. These spectra have been recorded at DP = 0 V. A typical CID spectrum for the $[Ca(\mathbf{TU})]^{2+}$ species is given in Figure 1. Note that

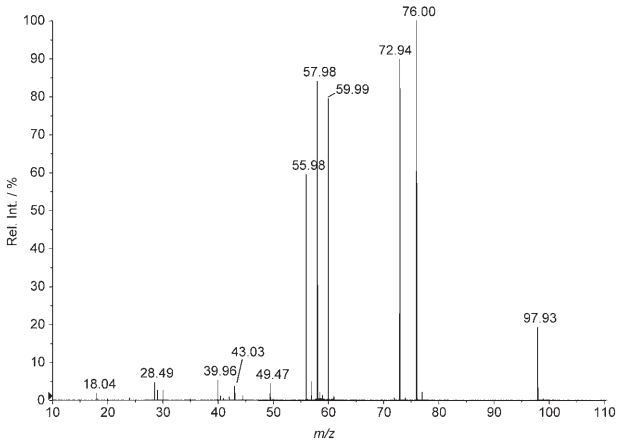

Figure 1. Low-energy CID spectrum of the $[Ca(thiourea)]^{2+}$ complex recorded at DP = 0 V and E_{lab} = 11 eV.

on our instrument and for this particular system, the smallest collision energy in the laboratory frame (E_{lab}) for which sufficient amount of fragment ions can reach the detector, is 8 eV, and at this value dissociation of the parent ions occurs quite extensively, its relative abundance being already about 61 %. E_{lab} was scanned from 8 to 14 eV. This corresponds to center-of-mass collision energies (E_{CM}) ranging from 3.11 to 5.44 eV, N_2 being used as target gas (see the corresponding breakdown graph given in Figure 1S of the Supporting Information). The $[Ca(\mathbf{TU})]^{2+}$ complex dissociates according to either neutral losses generating new dications, or through several Coulomb explosion processes. Like for urea, elimination of ammonia is observed, which gives rise to an ion at *m/z* 49.5. Two additional neutral molecules are eliminated. The first one is [H,N,C,S], giving rise to an ion at *m/z* 28.5. The second one corresponds to the loss of the intact thiourea, but the bare dication (*m/z* 20) is only observed for E_{lab} values greater than 11 eV (4.28 eV in the center-of-mass frame). All the other fragments observed in the MS/MS spectrum (namely *m/z* 18, 40, 43, 56, 60, 73, 76 and 98) arise from four distinct Coulomb explosion processes, that is, fragmentation of the $[Ca(\mathbf{TU})]^{2+}$ dication into two monocations. All the fragmentations are summarized in Scheme 1, together with the chemical formula postulated for each fragment ion.

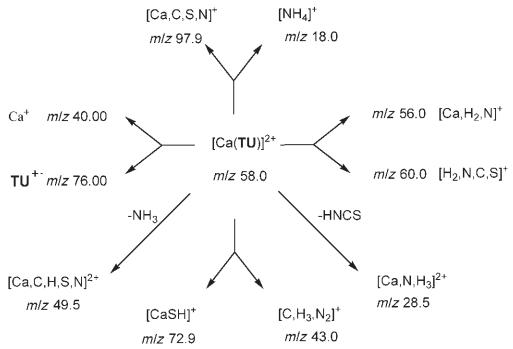

Scheme 1. Fragmentations of the $[Ca(\mathbf{TU})]^{2+}$ dication.

Unlike with urea, elimination of neutral molecules never prevails. For comparison, only two Coulomb explosions are observed with urea, which presently correspond to the 18/98 and 56/60 pairs. The most striking feature is the occurrence of a dissociative electron transfer between the ligand and the metallic center, giving rise to Ca^+ (*m/z* 40) and radical cation of thiourea (*m/z* 76.0). The fourth coulomb explosion, characteristic of this system leads to the calcium thiohydroxyl cation $[CaSH]^+$ at *m/z* 72.9 and concomitant formation of the organic ion $[C,H_3,N_2]^+$ (*m/z* 43).

Partner peaks arising from the Coulomb explosion processes should have in principle the same intensity. However, as it was already found for the urea–Ca^{2+} system, the lightest ions (*m/z* 18, 40, 43 and 58) are systematically less intense than the heaviest ones (*m/z* 98, 76, 73, 60, respectively). This effect is particularly pronounced for the three first pairs. Similar findings have been also previously reported for alcohols[51] and acetonitrile.[52] This phenomenon has been interpreted in terms of different radial ion energies, with the lighter ions generated by the Coulomb explosion gaining most of the radial energy and therefore having a much higher velocity than the relatively high mass ions. This can result in an unstable ion trajectory within the instrument and explains why lighter ions are detected in the MS/MS spectrum with smaller abundance. This effect may be even more pronounced in our QqTOF instrument, the lightest ions being less effectively transferred into the TOF region during the orthogonal injection step, because of their higher velocity.

Finally, note that the MS/MS spectra of all the singly-charged $[Ca(\mathbf{TU})_n{-}H]^+$ complexes have also been recorded. Their MS/MS spectra appear to be much simpler. The $[Ca(\mathbf{TU}{-}H)]^+$ ion MS/MS spectrum exhibits only fragment ions obtained by elimination of ammonia. The higher homologues are characterized by loss of up to $n-1$ thiourea units.

Structure and Bonding

The most stable $[Ca(\mathbf{TU})]^{2+}$ adduct, **1**, corresponds to a structure in which the metal dication is attached to the thiocarbonyl sulfur atom. It is worth noting that for both urea and thiourea the most basic site to protonation is the carbonyl[53] and the thiocarbonyl group,[54] respectively. At variance with urea, adduct **1** is only 2.9 kJ mol^{-1} lower in energy than form **2** in

which the metal dication bridges between the thiocarbonyl sulfur atom and one of the amino nitrogens (see Figure 2). Another important difference between both bases is that, while in the [Ca–urea]$^{2+}$ most stable complex, the metal dication lies in the same plane of the molecule, in [Ca(**TU**)]$^{2+}$ complex **1**, Ca^{2+} locates in the plane that bisects the NCN angle of the base and forms an angle of 120° with the C=S bond. The preference of bent structures for thioderivatives versus the preference of linear arrangements for the corresponding oxygen containing counterparts has been already reported for other metal monocations.[55] This is essentially a consequence of the different size of the basic center lone pairs. In the carbonyl group both lone pairs are small and the cation locates between both to enhance polarization effects. In thiocarbonyl groups the sulfur lone pairs are much larger and the specific interaction with a single lone pair is clearly favored.

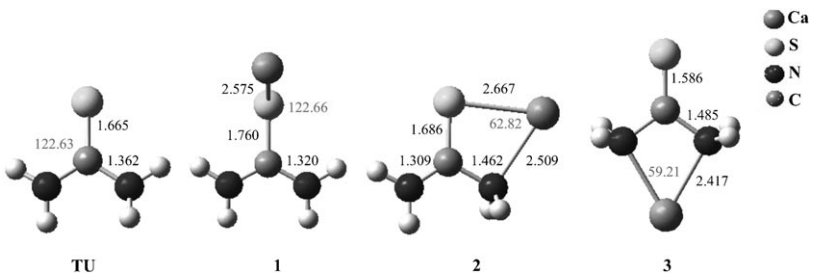

Figure 2. Optimized geometries for the most stable thiourea–Ca^{2+} adducts. Bond lengths are in Ångströms and bond angles in degrees. For the sake of comparison we have included also the optimized geometry of the isolated thiourea.

Similarly to what was found for urea,[29] a third local minimum, **3**, 128 kJ mol^{-1} less stable than **1**, corresponds to a complex in which Ca^{2+} bridges between both amino groups (see Figure 2).

Ca^{2+}–thiourea interactions are essentially electrostatic as revealed by the positive value of the energy density in the region between the two interacting subunits. It is worth noting however that the energy density contour maps for the two most stable adducts **1** and **2**, show a strong polarization of the valence shell density of sulfur toward the metal dication, and also of the nitrogen lone pair in the latter (see Figure 2S of the Supporting Information). This polarization affects directly the C=S bond, but it is transmitted also to the other bonds of the base. A comparison of the molecular graphs of neutral thiourea and the two most stable Ca^{2+}/thiourea complexes shows in both adducts, **1** and **2**, a decrease in the electron density at the C=S bond critical point, which lengthen by 0.095 and 0.019 Å, respectively. Concomitantly, in structure **1** the aforementioned polarization leads to an increase of the conjugation of the nitrogen lone-pair of the amino groups, which become strictly planar. Accordingly, the electron density at the C–N bond critical points (bcps) increases and the C–N bonds shorten by 0.041 Å. In complex **2**, the C–N bond directly interacting with the metal becomes significantly (0.054 Å) longer and the electron density at the bcp significantly smaller, whereas the other C–N bond becomes significantly reinforced, with a bond length 0.053 Å shorter and a greater electron density at the bcp. These changes are also reflected in the stretching frequencies. The C=S stretching frequencies in complexes **1** and **2** appear 83 and 41 cm^{-1} red-shifted, respectively with respect to the neutral compound. As far as the C–N stretching frequencies are concerned, they appear coupled as symmetric and antisymmetric combinations both in the neutral and in complex **1**, and are blue-shifted by 10 and 140 cm^{-1}, respectively. In complex **2** however, they are decoupled, that of the amino group interacting with the metal dication being significantly red-shifted, while that of the free amino group is blue-shifted.

Reaction Mechanisms for the Unimolecular Reactions of [Ca(U)]$^{2+}$ Complexes

As anticipated the potential energy surface (PES) corresponding to the unimolecular reactions of the [Ca(**TU**)]$^{2+}$ system is very complicated. Hence, for the sake of clarity we will discuss first that part of the PES with origin in the global minimum **1** (see Figure 3). The first conspicuous fact of Figure 3 is that the most favorable process from the global minimum **1** is its isomerization, through an internal rotation of the SCa group, to yield the second local minimum **2**. Hence, it is reasonable to admit that both have an almost equal significance as far as the unimolecular reactivity of [Ca(**TU**)]$^{2+}$ species is concerned. Hence, in the forthcoming sections we will also analyze in detail the PES with origin in this second local minimum.

In both Figures 3 and 4 we have distinguished the mechanisms associated with the loss of a neutral fragment (solid lines) from those which correspond to the formation of two monocations through Coulomb explosions (dashed lines).

Reaction Mechanisms with Origin in the Global Minimum 1

Besides the aforementioned isomerization yielding complex **2**, three other reaction pathways have their origin in minimum **1**: i) a 1,3-H shift from one amino group towards the sulfur atom yielding the structure **8** through the transition state **TS1 8**, ii) a symmetric displacement of Ca towards the plane containing the two amino nitrogen leading to the adduct **3**, iii) its coulomb explosion through the transition state **TS1 d** giving rise to Ca^{+} + thiourea$^{+\bullet}$.

Adduct **3** may also undergo a coulomb explosion, through an even lower activation barrier (**TS3 d**), to yield H_2NCa^{+} + H_2NCS^{+}, which correspond to the peaks detected at *m/z* 56 and 60, respectively in the CID spectra. H_2NCa^{+} can be also produced by the coulomb explosion of complex **8** (through **TS8 d**), the difference being the connectivity of the accompanying ion. Hence, according to our calculations, the *m/z* 60

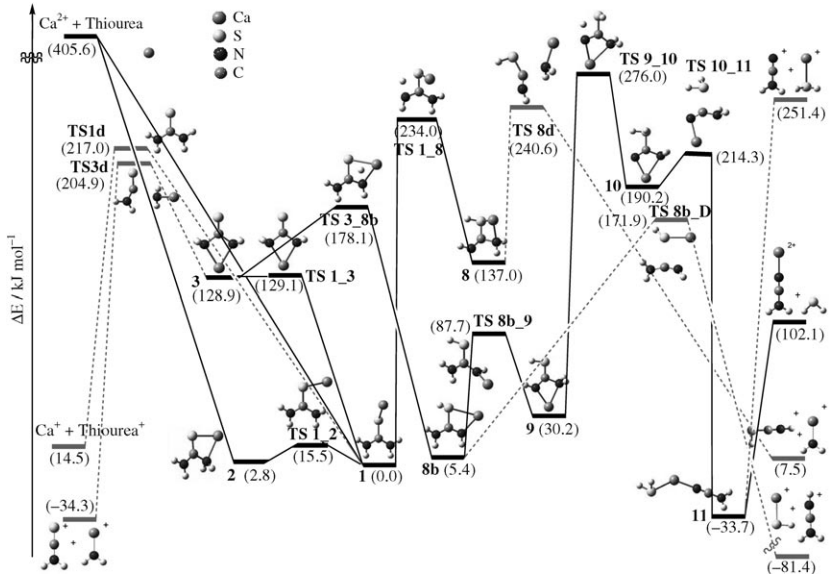

Figure 3. Energy profile of thiourea–Ca^{2+} reactions with origin in the most stable adduct **1**. Dashed lines correspond to mechanisms associated with Coulomb explosions.

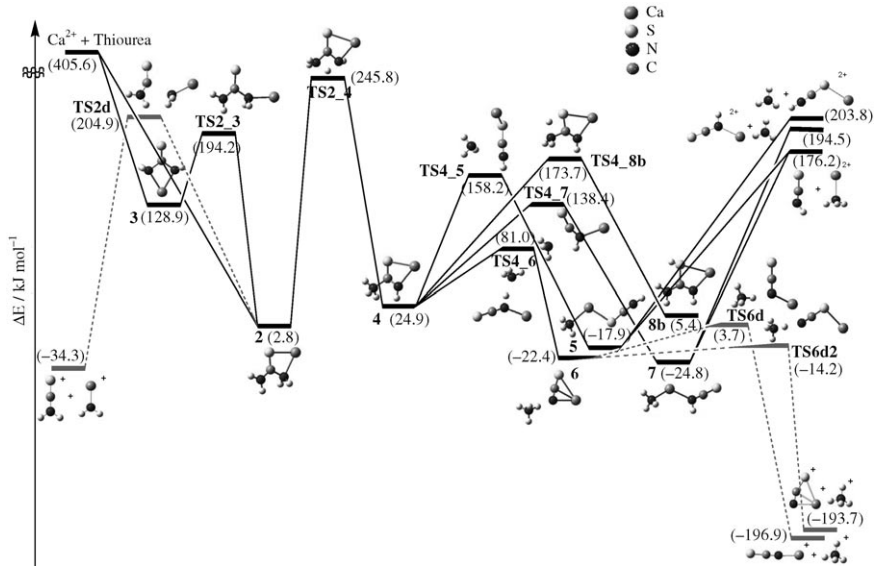

Figure 4. Energy profile of thiourea–Ca^{2+} reactions with origin in the second most stable adduct **2**. Dashed lines correspond to mechanisms associated with Coulomb explosions.

peak might correspond to two different ions, namely H_2NCS^+ and $HNCSH^+$, even though the former should be clearly dominant, because the corresponding process is more exothermic and the activation barrier associated with the coulomb explosion of species **3** is lower than that of species **8**.

Adduct **3**, may also evolve, through the **TS3 8b** transition state, to yield a quite stable local minimum **8b**. It is worth noting that this new minimum can be viewed as a conformer of species **8**. As a matter of fact, in **8** Ca interacts with both the sulfur atom and the amino group, whereas in **8b**, it bridges the sulfur atom and the imino group, accounting for its enhanced stability. More importantly, species **8b** yields in a quite exothermic coulomb explosion, through an activation barrier of 166 kJ mol^{-1}, the $CaSH^+ + H_2NCNH^+$ product ions observed experimentally. Actually, the peak corresponding to $CaSH^+$ (*m/z* 72.9) is among the more intense in the ESI spectra.

Minimum **8b**, may also finally yield, through the intermediates **9** and **10**, a very stable complex **11** in which the metal is connected to SH_2 and H_2NCN subunits. This species may dissociate either into $SH_2 + H_2NCNCa^{2+}$ or into $H_2SCa^+ + H_2NCN^+$ (the dissociation into $H_2SCa^{2+} + H_2NCN$, being 37.7 kJ mol^{-1} higher in energy). Both processes are quite endothermic with respect to **11**. Furthermore, the activation barrier to go from **9** to **10** is the highest of the whole PES, and therefore neither the loss of SH_2 nor the formation of H_2SCa^+ ions should be observed, in agreement with the experimental findings.

Reaction Mechanisms with Origin in Adduct 2

The local minimum **2** can be formed either by a direct attachment of Ca^{2+} to thiourea in a rather exothermic process or, as mentioned above, by isomerization from the global minimum through a very low activation barrier. Once complex **2** is formed, if one excludes the **2**→**1** interconversion, the most favorable process is its isomerization through an internal rotation of the NH_2–Ca moiety (see Figure 4), yielding the adduct **3** whose unimolecular reactivity was already discussed in the previous section. A little higher is the activation barrier associated with the coulomb explosion of **2** giving rise to the $H_2NCa^+ + H_2NCS^+$ singly-charged species. This mechanism is consistent with the significant activation of one of the C–N bonds in complex **2** discussed above. Hence, we can conclude that complex **2** would yield $H_2NCa^+ + H_2NCS^+$ either in a direct coulomb explosion, through the **TS2d** transition state or through a previous **2**→**3** isomerization (see Figure 3). Like for structure **1**, the less favorable process from **2** is a 1,3-H shift between the two amino groups, leading to complex **4**.

A bunch of processes arise from complex **4** (see Figure 4). The first two correspond to the cleavage of the C–NH_3 bond, leading to the formation of the very stable complexes **5** and **7**,

in which the NH_3 subunit initially bound to the C atom in structure **4** is now linked to Ca. These two complexes differ only by the atom of the HNCS moiety that is actually bonded to Ca (nitrogen in complex **7** or sulfur in complex **5**). These two complexes may lose either NH_3 or HNCS, leading to the two doubly-charged fragments $[Ca,H,N,C,S]^{2+}$ and $[Ca(NH_3)]^{2+}$, respectively, that are indeed observed experimentally in the MS/MS spectrum, at *m/z* 49.5 and 28.5, respectively. Since there was some controversy in the literature about the existence of metal dications solvated by a single molecule of water or ammonia,[5,6,28,56,57] it is worth noting that in these processes the doubly charged species $[Ca(NH_3)]^{2+}$ is indeed generated, which provides further evidence for the existence of a Ca^{2+} dication solvated by only one molecule of ammonia in the gas phase.[58] This species was already detected in the study of the Ca^{2+}/urea system.[29] It is also worth noting that these fragmentations in which a doubly charged species is formed can be viewed as a Cooks kinetic experiment.[59,60] Hence, the dissociation of complex **5** or **7** into $[Ca(NH_3)]^{2+}$ and $[CaSCNH]^{2+}$ or $[Ca(H)NCS]^{2+}$, respectively, clearly show that the Ca^{2+} affinity of ammonia is greater than that of HNCS, regardless of the attachment site of the metal to the HNCS moiety. Our data also show that HNCS behaves preferentially as a nitrogen base towards Ca^{2+}.

Figure 4 also shows that the most favorable process occurring from **4**, is the formation of the intermediate **6**, in which a NH_4^+ ion is hydrogen bonded to a $NCSCa^+$ fragment, as reflected in its molecular graph (see Figure 1S of the Supporting Information) that shows the existence of a bond critical point between one of the hydrogen atoms of the NH_4^+ moiety and the N atom of the $NCSCa^+$ subunit, while the net charge of both subunits is practically +1 (+0.98 and +1.02, respectively). This weakly bound species undergoes two different coulomb explosions, which differ in the connectivity of the ion that accompanies NH_4^+. In the most exothermic one Ca is attached to the nitrogen atom of the NCS entity, which is its most basic site. In the less exothermic, Ca is bound to the sulfur atom. These two coulomb explosions account for the formation of the ions at *m/z* 18 and 97.9. The latter one should therefore correspond to a mixture of two structures, even if one may reasonably assume that the population of $[CaNCS]^+$ should be dominant.

Finally, the last process involving the adduct **4** gives rise to the intermediate **8b**, which, as previously described, may evolve towards the formation of $HSCa^+$ (*m/z* 72.9) and H_2NCNH^+ (*m/z* 43).

Analogies and Dissimilarities between Urea–Ca^{2+} and Thiourea–Ca^{2+} Reactions

The overall topology of the thiourea–Ca^{2+} PES is in agreement with the experimental observations. MS/MS spectra were recorded at a collision energy ranging from 8 to 14 eV in the laboratory frame. This corresponds to center-of-mass collision energies starting from 3.11 eV. Interestingly, the fact that all the product ions are already detected at the lowest collision energy is consistent with the energetics associated of the various reactions pathways considered in Figures 3 and 4. It is also worth noting that bare Ca^{2+} ions at *m/z* 20 start to be detected for center-of-mass collision energies higher than 4 eV, which merely corresponds to the calculated binding energy for **TU** (404 kJ mol^{-1}). The intensity of Ca^{2+} remains very small as the collision energy is further increased, as can be observed in the breakdown graph given in Figure 1S of the Supporting Information.

The highest barriers associated with the various coulomb explosions are typically in the 201–230 kJ mol^{-1} range. The lowest energy paths are those yielding to NH_2Ca^+ and $CaSH^+$, then followed by those leading to Ca^+ and NH_4^+, which are also observed for the urea/Ca^{2+} system. In addition, both the loss of NH_3 and HNCS are very minor processes. This is consistent with the fact that they originate from the suitable precursors **5** and **7**, and therefore require more energy than the proton transfer leading to the NH_4^+ moiety in complex **6**. This is at variance with respect to the $[Ca(urea)]^{2+}$ unimolecular reactivity, where the energy requirements to form NH_4^+ ion or to lose NH_3, are rather similar, explaining that the loss of NH_3 is more important in the urea case.

Another interesting difference between urea–Ca^{2+} and thiourea–Ca^{2+} reactions is that the dissociative charge transfer leading to Ca^+ and the ionized ligand, is a favorable process for the Ca^{2+}/thiourea system, as attested by the intense peak at *m/z* 76 ($\mathbf{TU}^{+\cdot}$), while such a charge transfer is not observed with urea. This dissimilarity between urea and thiourea undoubtedly reflects the large difference in their ionization energies (10.27 to 8.50 eV, respectively),[61] the charge transfer being thermodynamically favorable only in the case of thiourea.

The third important difference between urea–Ca^{2+} and thiourea–Ca^{2+} reactions is that while the coulomb explosion yielding $CaSH^+ + H_2NCNH^+$ is very favorable for the latter, a similar process (formation of $CaOH^+ + H_2NCNH^+$) is not observed for urea. This may be explained by the substantial difference between the barriers associated with the hydrogen shifts from the amino groups towards the carbonyl (thiocarbonyl) group. In thiourea these hydrogen shifts involve activation barriers that are rather similar to those of the different coulomb explosions and to those of the hydrogen shifts between the amino groups. Conversely, in urea, these barriers are much higher in energy, and therefore the associated processes very unfavorable. This actually reflects the fact that a carbonyl bond is stronger than a thiocarbonyl one, while a S–H bond is weaker than an O–H bond, the first effect being dominant as it has been shown by comparing the atomization energies of thioformaldehyde + methanol with the atomization energies of formaldehyde + thiomethanol.[62,63] Consistently, the thiocarbonyl–thioenol enthalpy difference is much smaller than the carbonyl–enol enthalpy difference,[64] so while the formation of a S–H bond in thiourea reactions is energetically accessible, the formation of an O–H bond in urea is not.

Conclusions

The gas-phase unimolecular reactivity Ca^{2+} ions towards urea and thiourea share several common features as well as significant dissimilarities. In both processes, the formation of new doubly charged species, namely $[Ca,H,N,C,S]^{2+}$ (or $[Ca,H,N,C,O]^{2+}$) and $[Ca(NH_3)]^{2+}$ by the loss of NH_3 and HNCS (or HNCO), respectively, are observed. However, while these processes are dominant with urea, they only occur to a minor extent with thiourea. The H_2NCa^+ and NH_4^+ monocations are also observed in both systems, as a result of typical coulomb explosion processes. In the particular case of the Ca^{2+}/thiourea system, two new coulomb explosions are observed, yielding $Ca^+ + \text{thiourea}^{+\cdot}$ and $HSCa^+ + H_2NCNH^+$, respectively. The first is attributed to the ionization energy of thiourea, which is significantly lower than that of urea. The second is a consequence of the fact that, as shown previously in the literature,[62] thioenols are intrinsically more stable than enols with respect to the corresponding keto forms. Consequently, the H-shift processes from the amino group toward the carbonyl (thiocarbonyl) group which in urea are very unfavorable become energetically accessible for thiourea and are characterized by activation energies similar to those involved in H-shifts between the amino groups.

Acknowledgements

This work has been partially supported by the DGI Project No. BQU2003–00894, by the COST Action D26/0014/03 and by the Project MADRISOLAR, Ref.: S-0505/PPQ/0225 of the Comunidad Autónoma de Madrid. A generous allocation of computing time at the CCC of the UAM is also acknowledged.

Keywords: cations · coulomb explosions · density functional calculations · gas-phase · thiourea

[1] M. Beyer, E. R. Williams, V. E. Bondybey, *J. Am. Chem. Soc.* **1999**, *121*, 1565 – 1573.
[2] S. Petrie, L. Radom, *Int. J. Mass Spectrom.* **1999**, *192*, 173 – 183.
[3] D. Schröder, H. Schwarz, *J. Phys. Chem. A* **1999**, *103*, 7385 – 7394.
[4] B. Song, J. Zhao, R. Griesser, C. Meiser, H. Sigel, B. Lippert, *Chem. Eur. J.* **1999**, *5*, 2374 – 2387.
[5] A. M. El-Nahas, N. Tajima, K. Hirao, *Chem. Phys. Lett.* **2000**, *318*, 333 – 339.
[6] D. Schröder, H. Schwarz, J. Wu, C. Wesdemiotis, *Chem. Phys. Lett.* **2001**, *343*, 258 – 264.
[7] A. M. El-Nahas, *Chem. Phys. Lett.* **2002**, *365*, 251 – 259.
[8] A. A. Shvartsburg, J. G. Wilkes, *J. Phys. Chem. A* **2002**, *106*, 4543 – 4551.
[9] H. Cox, G. Akibo-Betts, R. R. Wright, N. R. Walker, S. Curtis, B. Duncombe, A. J. Stace, *J. Am. Chem. Soc.* **2003**, *125*, 233 – 242.
[10] N. Russo, M. Toscano, A. Grand, *J. Phys. Chem. A* **2003**, *107*, 11533 – 11538.
[11] A. A. Shvartsburg, J. G. Wilkes, *Int. J. Mass Spectrom.* **2003**, *225*, 155 – 166.
[12] N. R. Walker, G. A. Grieves, J. B. Jaeger, R. S. Walters, M. A. Duncan, *Int. J. Mass Spectrom.* **2003**, *228*, 285 – 295.
[13] D. Asthagiri, L. R. Pratt, M. E. Paulaitis, S. B. Rempe, *J. Am. Chem. Soc.* **2004**, *126*, 1285 – 1289.
[14] H. Cox, A. J. Stace, *J. Am. Chem. Soc.* **2004**, *126*, 3939 – 3947.
[15] R. B. Metz, *Int. J. Mass Spectrom.* **2004**, *235*, 131 – 143.
[16] J. Poater, M. Sola, A. Rimola, L. Rodríguez-Santiago, M. Sodupe, *J. Phys. Chem. A* **2004**, *108*, 6072 – 6078.
[17] D. Schröder, *Angew. Chem.* **2004**, *116*, 1351 – 1353; *Angew. Chem. Int. Ed.* **2004**, *43*, 1329 – 1331.
[18] T. J. Shi, G. Orlova, J. Z. Guo, D. K. Bohme, A. C. Hopkinson, K. W. M. Siu, *J. Am. Chem. Soc.* **2004**, *126*, 7975 – 7980.
[19] N. G. Tsierkezos, D. Schröder, H. Schwarz, *Int. J. Mass Spectrom.* **2004**, *235*, 33 – 42.
[20] R. L. Wong, K. Paech, E. R. Williams, *Int. J. Mass Spectrom.* **2004**, *232*, 59 – 66.
[21] C. Y. Xiao, K. Walker, F. Hagelberg, A. M. El-Nahas, *Int. J. Mass Spectrom.* **2004**, *233*, 87 – 98.
[22] M. Belcastro, T. Marino, N. Russo, M. Toscano, *J. Mass Spectrom.* **2005**, *40*, 300 – 306.
[23] B. J. Duncombe, L. Puskar, B. H. Wu, A. J. Stace, *Can. J. Chem.* **2005**, *83*, 1994 – 2004.
[24] S. Guillaumont, J. Tortajada, J. Y. Salpin, A. M. Lamsabhi, *Int. J. Mass Spectrom.* **2005**, *243*, 279 – 293.
[25] T. J. Shi, J. F. Zhao, A. C. Hopkinson, K. W. M. Siu, *J. Phys. Chem. B* **2005**, *109*, 10590 – 10593.
[26] E. Rincon, P. Jaque, A. Toro-Labbe, *J. Phys. Chem. A* **2006**, *110*, 9478 – 9485.
[27] I. Tunell, C. Lim, *Inorg. Chem.* **2006**, *45*, 4811 – 4819.
[28] A. Palacios, I. Corral, O. Mó, F. Martin, M. Yáñez, *J. Chem. Phys.* **2005**, *123*.
[29] I. Corral, O. Mó, M. Yáñez, J.-Y. Salpin, J. Tortajada, L. Radom, *J. Phys. Chem. A* **2004**, *108*, 10080 – 10088.
[30] I. Corral, O. Mó, M. Yáñez, J. Y. Salpin, J. Tortajada, D. Moran, L. Radom, *Chem. Eur. J* **2006**, *12*, 6787 – 6796.
[31] H. Basch, M. Krauss, W. J. Stevens, *J. Am. Chem. Soc.* **1985**, *107*, 7267 – 7271.
[32] J. J. R. Fraudo da Silva, R. J. P. Williams, *The Biological Chemistry of Elements*, Oxford University Press, Oxford, **1991**.
[33] H. Sigel, *Chem. Soc. Rev.* **1993**, *22*, 255 – 267.
[34] S. Forsen, J. Kordel, *Bioinorganic Chemistry*, University Science Books, Mill Valley, California, **1994**.
[35] Y. V. Bukhman, D. E. Draper, *J. Mol. Biol.* **1997**, *273*, 1020 – 1031.
[36] B. K. Garg, U. Burman, S. Kathju, *Plant Growth Regulation* **2006**, *48*, 237 – 245.
[37] B. Z. Zhu, W. E. Antholine, B. Frei, *Free Radical Biol. Med.* **2002**, *32*, 1333 – 1338.
[38] M. Akagawa, K. Suyama, *Free Radical Res.* **2002**, *36*, 13 – 21.
[39] H. Takahashi, A. Nishina, R. Fukumoto, H. Kimura, M. Koketsu, H. Ishihara, *Life Sci.* **2005**, *76*, 2185 – 2192.
[40] M. van Zeijl, J. Fairhurst, T. R. Jones, S. K. Vernon, J. Morin, J. LaRocqe, B. Feld, B. O'Hara, J. D. Bloom, S. V. Johann, *J. Virology* **2000**, *74*, 9054 – 9061.
[41] T. K. Venkatachalam, E. A. Sudbeck, C. Mao, F. M. Uckun, *Bioorg. & Med. Chem. Letters* **2001**, *11*, 523 – 528.
[42] R. J. Visalli, J. Fairhurst, S. Srinivas, W. Hu, B. Feld, M. DiGrandi, K. Curran, A. Ross, J. D. Bloom, M. van Zeijl, T. R. Jones, J. O'Connell, J. I. Cohen, *J. Virology* **2003**, *77*, 2349 – 2358.
[43] I. Corral, O. Mó, M. Yáñez, A. Scott, L. Radom, *J. Phys. Chem. A* **2003**, *107*, 10456 – 10461.
[44] A. D. Becke, *J. Chem. Phys.* **1993**, *98*, 1372 – 1377.
[45] C. Lee, W. Yang, R. G. Parr, *Phys. Rev. B* **1988**, *37*, 785 – 789.
[46] M. A. Iron, M. Oren, J. M. L. Martin, *Mol. Phys.* **2003**, *101*, 1345 – 1361.
[47] M. B. Sullivan, M. A. Iron, P. C. Redfern, J. M. L. Martin, L. A. Curtiss, L. Radom, *J. Phys. Chem. A* **2003**, *107*, 5617 – 5630.
[48] A. P. Scott, L. Radom, *J. Phys. Chem.* **1996**, *100*, 16502 – 16513.
[49] Gaussian 03, Revision B.05, M. J. Frisch, G. W. Trucks, H. B. Schlegel, G. E. Scuseria, M. A. Robb, J. R. Cheeseman, V. G. Zakrzewski, J. J. A. Montgomery, T. Vreven, K. N. Kudin, J. C. Burant, J. M. Millam, S. S. Iyengar, J. Tomasi, V. Barone, B. Mennucci, M. Cossi, G. Scalmi, N. Rega, G. A. Petersson, H. Nakatsuji, M. Hada, M. Ehara, K. Toyota, R. Fukuda, J. Hasegawa, M. Ishida, T. Nakajima, Y. Honda, O. Kitao, C. Adamo, J. Jaramillo, R. Gomperts, R. E. Stratmann, O. Yazyev, J. Austin, R. Cammi, C. Pomelli, J. Ochterski, P. Y. Ayala, K. Morokuma, G. A. Voth, P. Salvador, J. J. Dannenberg, V. G. Zakrzewski, S. Dapprich, A. D. Daniels, M. C. Strain, O. Farkas, D. K. Malick, A. D. Rabuck, K. Raghavachari, J. B. Foresman, J. V. Ortiz, Q. Cui, A. G. Baboul, S. Clifford, J. Cioslowski, B. B. Stefanov, G. Liu, A. Liashenko, P. Piskorz, I. Komaromi, R. L. Martin, D. J. Fox, T. Keith, M. A. Al-Laham, C. Y. Peng, A. Nanayakkara, M. Challacombe, P. M. W. Gill, B.

Johnson, W. Chen, M. W. Wong, C. Gonzalez, J. A. Pople, Gaussian, Inc., Wallingford CT, **2003**.
[50] R. F. W. Bader, *Atoms in Molecules. A Quantum Theory*, Clarendon Press, Oxford, **1990**.
[51] J. Kohno, F. Mafune, T. Kondow, *J. Phys. Chem. A* **1999**, *103*, 1518 – 1522.
[52] H. Studer, H. Kohler, H. Bürgi, C. Binswanger, J. Steiger, *Endocrinology* **1972**, *91*, 1154 – 1159.
[53] F. Wang, S. Ma, D. Zhang, R. G. Cooks, *J. Phys. Chem. A* **1998**, *102*, 2988 – 2994.
[54] J. L. M. Abboud, O. Mó, J. L. G. de Paz, M. Yáñez, M. Esseffar, W. Bouab, M. El-Mouhtadi, R. Mokhlisse, E. Ballesteros, M. Herreros, H. Homan, C. Lopezmardomingo, R. Notario, *J. Am. Chem. Soc.* **1993**, *115*, 12468 – 12476.
[55] M. Alcamí, O. Mó, M. Yáñez in *Modeling Intrinsic Basicities: The Use of the Electrostatic Potentials and the Atoms-in-Molecules Theory, Vol. 3* (Eds.: J. S. Murray, K. Sen), Elsevier, Amsterdam, **1996**, pp. 407 – 456.
[56] A. J. Stace, N. R. Walker, R. R. Wright, S. Firth, *Chem. Phys. Lett.* **2000**, *329*, 173 – 175.
[57] A. A. Shvartsburg, K. W. M. Siu, *J. Am. Chem. Soc.* **2001**, *123*, 10071 – 10075.
[58] It should be mentioned that although the $HNCS^+ + CaNH_3^+$ dissociation limit is lower than the $HNCS + [CaNH_3]^{2+}$, both complexes **5** and **7** dissociate diabatically into $HNCS + Ca[NH_3]^{2+}$, while their dissociation into $HNCS^+ + CaNH_3^+$ requires a very high activation barrier through a conical intersection that lies 360 $kJ\,mol^{-1}$ above local minimum **7** as estimated in CASSCF(4,4)/6–31G* level of theory.
[59] S. A. McLuckey, D. Cameron, R. G. Cooks, *J. Am. Chem. Soc.* **1981**, *103*, 1313 – 1317.
[60] R. G. Cooks, J. S. Patrick, T. Kotiaho, S. A. McLuckey, *Mass Spectrom. Rev.* **1994**, *13*, 287 – 339.
[61] *NIST Chemistry Webbook: Standard Reference Database Number 69*. (Eds. P. J. Linstrom, W. G. Mallard), National Institute of Standards and Technology, Gaithersburg MD, p. 20899 (http://webbook.nst.gov), **2005**.
[62] L. Gonzalez, O. Mó, M. Yáñez, *J. Phys. Chem. A* **1997**, *101*, 9710 – 9719.
[63] M. Lamsabhi, M. Alcami, O. Mó, W. Bouab, M. Esseffar, J. L. M. Abboud, M. Yáñez, *J. Phys. Chem. A* **2000**, *104*, 5122 – 5130.
[64] S. Sklenak, Y. Apeloig, Z. Rappoport, *J. Chem. Soc., Perkin Trans. 2* **2000**, 2269 – 2279.

Received: February 14, 2007
Revised: April 10, 2007
Published online on May 10, 2007

